

Numerical investigation of the gel barrier formation with vertical injection pipe

Meejeong Kim · M. Yavuz Corapcioglu ·
Jae-Woo Park

Received: 17 January 2007 / Accepted: 6 February 2007 / Published online: 21 February 2007
© Springer-Verlag 2007

Abstract Permeation grouting is the injection of a fluid grout into ground and production of a solidified mass to carry increased load and/or fill voids to control water flow. This study examined a technology of constructing horizontal gel barrier by the permeation grouting through multiple vertical injection pipes. Colloidal Silica (CS) solution was used as a gelling liquid to be injected and solidified in the unsaturated soil. Formation of a gel bulb was simulated and the results were compared with those obtained from the sleeve pipe injection with horizontal pipes. The gel bulb generated from the injection method employing vertical pipe showed greater sensitivity of the bulb's lateral extent to variations in operating conditions compared to the sleeve pipe injection. Although in the limited numbers, in all examined cases, the vertical-pipe system appeared to consume a larger volume of CS solution than the horizontal-pipe system to form an equivalent horizontal gel barrier. This result supports our intuition that the injection with the horizontal pipes may be more effective than the one with vertical pipes in constructing horizontal gel barrier.

Keywords Barrier · Colloidal silica · Permeation grouting · Numerical model · Unsaturated soil

M. Kim · J.-W. Park (✉)
Department of Civil Engineering,
Hanyang University,
Seoul 133-791, South Korea
e-mail: jaewoopark@hanyang.ac.kr

M. Y. Corapcioglu
Department of Civil Engineering,
Texas A&M University,
College Station, TX 77843, USA

Introduction

The installation of containment systems can be used as an integral part of in situ remediation when other remediation technologies are cost-prohibitive or unsatisfactory. A gelling liquid-based barrier can be installed in high-permeability soils by permeation grouting when subsurface excavation for the containment systems such as slurry trenches is difficult. The permeation grouting technology involves the injection of a gelling liquid which initially has a low viscosity into the subsurface at low pressure not exceeding the soil fracture pressure. The liquid injected finally gels to plug the pore spaces and achieve low permeabilities.

This barrier installation technique has some advantages such as: low cost, no disturbance of wastes, and capability of emplacing vertical or horizontal barriers. Its disadvantages are that application is limited to formations with moderate to high permeabilities, and prediction of penetrated grout radius and ensurance of continuity are difficult (Pearlman 1999). In general, injection of a low-viscosity gelling liquid at low pressure is accomplished by two main methods: point injection and sleeve pipe injection (tube-a'-manchette). In the point injection method, a casing is driven to full depth and is withdrawn as grout is injected. The sleeve pipe injection involves grout injection through holes placed at 30-cm intervals along the pipe.

A non-toxic and inert gelling liquid, Colloidal Silica (CS), has been investigated as a potential gelling liquid to form a subsurface barrier (Noll et al. 1992; Finsterle et al. 1994; Moridis et al. 1999; Kim and Corapcioglu 2002a, 2002b). CS barrier technology has been applied at Brooklin National Laboratory on Long Island, New York (Heiser et al. 2000). The advantages of CS gel

system can be summarized as low permeability ($< 10^{-11}$ cm²), controllable gel time, high injectivity, minimal environmental impacts, and no syneresis and degradation process by bacteria (Jurinak and Summers 1991; Yonekura and Kaga 1992).

Numerical models designed to simulate CS solution injection were presented by Finsterle et al. (1994), Kim and Corapcioglu (2002a). Moridis et al. (1999) used the numerical model presented by Finsterle et al. (1994) to evaluate design options for the placement of gel barrier. Kim and Corapcioglu (2002b) investigated the construction of horizontal gel barrier for effective prevention of contaminant migration in unsaturated soil, by injecting CS solution through the holes in multiple horizontal pipe.

This study investigates installation of the horizontal gel barrier by injecting CS solution through multiple vertical pipes. The idea is that the vertical pipes are placed in a zigzag fashion and CS solution is injected from each pipe at certain depth so as to allow a gel bulb generated by the point injection from each pipe to overlap each other and then form a horizontal gel plane (Figs. 1, 2). This point injection method is differentiated than what is usually done, i.e., withdrawing the pipe as injecting a gelling liquid. This study aims to compare the performance of the injection method using vertical pipes to those using horizontal pipes in the formation of horizontal barrier in the unsaturated soil (Kim and Corapcioglu 2002b), and to investigate the feasibility of the vertical-pipe injection method.

Numerical experiments

Mathematical model

The most unique aspect of the migration of a gelling solution compared with a conventional fluid flow in

Fig. 1 An illustrative example of a system with multiple vertical injection pipes. **a** Three pipes are installed at the points ($x = 0, y = 0$), ($x = 5\text{cm}, y = 5\text{cm}$), and ($x = -5\text{cm}, y = 5\text{cm}$), respectively, and CS is injected at the bottom of each pipe at $z = 0$. **b** Reduction of an intrinsic permeability (which is defined as $1 - k_{0n}/k_n$). The soil properties and operating parameters used in the simulation are listed in Tables 1 and 2

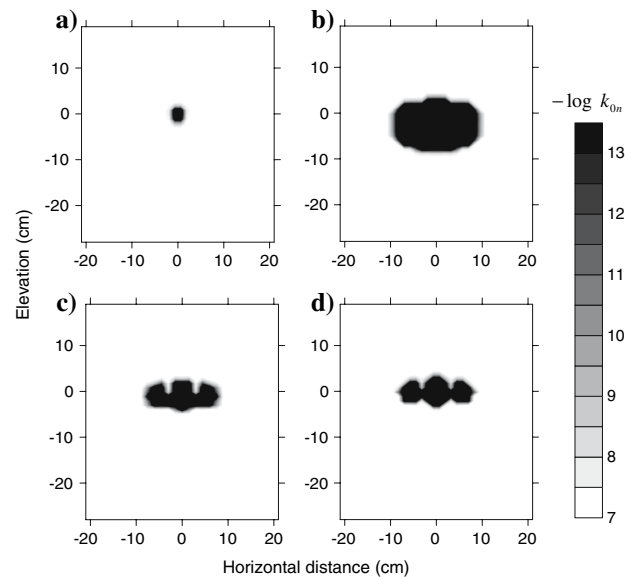
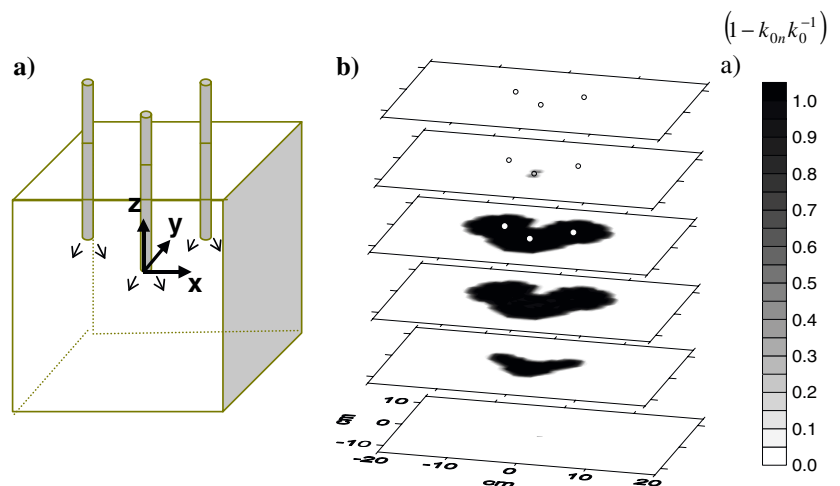


Fig. 2 Cross-sectional profiles of the intrinsic permeability in negative logarithmic scale. **a** reference case; **b** case when the soil has 10 times the higher intrinsic permeability; **c** case when the gel time is increased about 3 times; **d** case when the injection pressure is increased 5 times. The dark area represents the CS gel-saturated area

porous media is that the solution viscosity continuously increases and the solution finally ceases to move. This study uses the model presented by Kim and Corapcioglu (2002a) to simulate the placement of gelling liquid in unsaturated soils. In this model, the sol and gel phases are individually quantified and the solution viscosity is calculated from the numerical solutions of governing equations: They discovered a unique normalized viscosity curve from the viscosity measurements at different gelation rates, and established a dependency of the viscosity on the volumetric fraction of the gel phase by combining a kinetic gelation model

and the normalized viscosity curve. This is based on the fact that the solution is occupied with the larger fraction of gel phase as the gelation proceeds and hence the solution viscosity increases.

The model developed consists of mass balance equations in which gelation is incorporated through reaction terms, and auxiliary equations including a correlation of viscosity to the volumetric fraction of gel phase. The basic assumptions made in developing the mathematical model are: (1) CS solution is miscible and thus mixes with water, forming a gel mixture; (2) the gel mixture consists of two phases, i.e., sol phase (a suspension of discrete colloidal silica particles in water) and gel phase (cross-linked colloidal silica particles and the captured water inside their chain-like structure); (3) there is no capillary force between the two phases, and thus they migrate together; (4) their movements are governed by the gel mixture properties such as gel mixture density, viscosity, and pressure.

A brief description of the gelation model follows: The rate of gelling reaction was assumed to be rewritten as

$$\frac{dF_s}{dt} = -k_1 F_s (F_s C_{cs} + F_g C_{cg}) = -k_1 F_s C_{c0} \tag{1}$$

for a closed system where no dilution is involved. where k_1 is a gelation rate coefficient, F_s and F_g respectively represent volumetric fractions of the sol phase and gel phase in the gel mixture, C_{cs} and C_{cg} are the colloidal silica concentrations in the sol phase and gel phase, respectively. C_{c0} is colloidal silica concentration of the injected CS solution.

If a general single reaction with a stoichiometric equation $F_s \rightarrow F_g$ is considered, the gel phase volumetric fraction F_g and time t are related by

$$t = -\frac{\ln [(F_{s0} + F_{g0} - F_g)/F_{s0}]}{k_1 C_{c0}} = -\frac{\ln (1 - F_g)}{k_1 C_{c0}}. \tag{2}$$

The initial gel phase volumetric fraction F_{g0} is zero, and the initial sol phase volume fraction F_{s0} is one.

A gelation rate coefficient k_1 can be determined by measuring the half-time $t_{0.5}$ (i.e., the time when the gel volume fraction reaches 0.5, which is also called the gel-point) and by using Eq. 2. The gel-point $t_{0.5}$ can be determined graphically by the intersection of a straight line through the initial baseline viscosity and a line through the plotted viscosity versus time data where the viscosity shows a rapid increase (Kim and Corapcioglu 2002a). From the viscosity measurements ranging over several orders of magnitude, the gel-point can be easily located by observing the time when the viscosity starts to increase rapidly.

According to Eq. 2, the gelation rate constant is determined by

$$k_1 = \frac{\ln 0.5}{-t_{0.5} C_{c0}}. \tag{3}$$

From $t_{0.5}$ values for different NaCl concentrations, the dependence of k_1 on the NaCl concentration is obtained as given by

$$k_1 = 1.85 \times 10^{10} C_{NaCl}^7, \tag{4}$$

where C_{NaCl} is the NaCl concentration in the gel mixture. Once the reaction rate coefficient–NaCl concentration relationship is established, the gel-point can be estimated for any CS solution by using Eqs. 3 and 4 with different NaCl concentrations. It is noted that this expression was obtained as the best fit of the data in practical range of NaCl concentration, not based on any theoretical approach.

The gel mixture viscosity is affected when migrating in the subsurface by dilution due to the pore water. By Kim and Corapcioglu (2002a), the gel mixture viscosity, μ_m , is related to the volumetric fraction of the gel phase, F_g , as given by

$$\mu_m = \mu_s - 0.3[\exp(0.734)]^{0.01} + 0.3\left\{\exp\left[0.734(1 - F_g)^{\frac{6.5}{\ln 0.5}}\right]\right\}^{0.01}, \tag{5}$$

where μ_s is the viscosity contributed by the sol phase, which is given by Eq. 6 that employs a power-mixing rule (Koval 1963)

$$\mu_s = \left(\frac{X}{\mu_0^{1/4}} + \frac{1 - X}{\mu_w^{1/4}}\right)^{-4}, \tag{6}$$

where μ_w is the water viscosity, μ_0 is the viscosity of the injected CS solution, and X is the volumetric fraction of injected CS solution in the sol phase.

Ion exchange between the solution and subsurface may occur during the CS solution flows in the subsurface, which leads uncontrolled gelation and unsatisfactory results. This model, however, does not consider geochemical reactions between the CS solution and the subsurface assuming a condition where there is a negligible interaction between the CS solution and the subsurface. Using a surface-modified CS (Nyacal DP5110) or preflushing the subsurface prior to the injection of CS solution can prevent the ion exchange between the solution and subsurface, and hence ultimately uncontrolled gelation and unsatisfactory results (Moridis et al. 1999).

Verification of numerical model

The governing equations were developed in cylindrical coordinates to demonstrate the radial symmetry of the CS solution migration through a single vertical pipe (Fig. 2a). An alternative direction implicit finite difference method was used to solve the governing equations. Non-linearities of the algebraic equations were handled by an iterative method. At each iterative cycle the tridiagonal matrix generated from a set of algebraic equations for all nodes was solved by the Thomas Algorithm. Non-uniform grid sizes were used, and time steps were designed to gradually increase as the gel mixture migration slows down with time.

The capability of the mathematical model was previously verified by conducting column tests and comparing the model predictions with the experimental data in Kim and Corapcioglu (2002a). Two-dimensional (2-D) axisymmetric numerical model developed in this study was verified by comparing its solutions to the numerical solutions obtained from the SWMS_2D code (Simunek et al. 1994). The code numerically solves the Richard's equation for saturated–unsaturated water flow and the advection–dispersion equation for solute transport using the Galerkin finite-element method with linear basis functions. Among the example problems presented in the code, the one simulating variably saturated water flow and solute transport in a three-dimensional region exhibiting axisymmetry about a vertical axis was used for the model verification. Modification to its input data was made to provide the same boundary conditions as those of the model developed as shown in Eqs. 7 and 8. The constant pressure head and concentration were given at nodes $r = 0 - 7$ cm, $z = 0$, and uniform distribution of water content was assumed as the initial condition. The same nodal structure was also given for both numerical models compared. The soil hydraulic and solute transport parameters used in the simulations are listed in Tables 1 and 2. Figure 2b,c presents water content and concentration profiles, respectively, at the end of the simulation (=5 min). Good agreements are obtained between SWMS_2D and the model developed, indicating the flow and solute transport phenomena were correctly represented in the numerical model.

Boundary and initial conditions

For all simulations no-flux condition was specified along the left and top boundaries, and zero-gradient conditions were prescribed along the right and bottom boundaries. Constant pressure head and concentration

Table 1 Soil properties used in numerical experiments

Parameters	Values
θ_s , Water content at full saturation	0.39
θ_r , Water content at residual saturation	0.01
α , Parameter in the saturation–capillary relation	0.13 cm^{-1}
a , Parameter in the saturation–capillary relation	5
b , Parameter in the saturation–capillary relation	0.8
k_0 , Intrinsic soil permeability	$2.04 \times 10^{-6} \text{ cm}^2$

were given at nodes representing injection points. The initial and boundary conditions for all simulations are expressed as

$$h_m = H_0, \quad t = 0, \quad 0 \leq r \leq r_u, \quad z_l \leq z \leq z_u, \quad (7a)$$

$$t = 0, \quad 0 \leq r \leq r_u, \quad z_l \leq z \leq z_u$$

$$q_{mr} = 0, \quad t > 0, \quad r = 0, \quad r = r_u, \quad (7b)$$

$$\frac{\partial h_m}{\partial z} = 0, \quad t > 0, \quad z = z_l, \quad (7c)$$

$$q_{mz} = 0, \quad t > 0, \quad z = z_u, \quad (7d)$$

$$q_{mr} = q_{mz} = 0, \quad t > 0, \quad \text{at the pipe}, \quad (7e)$$

$$h_m = H_i, \quad t > 0, \quad \text{at the injection point}, \quad (7f)$$

$$F_s = 1, \quad C_{cs} = C_{cg} = 0, \quad t = 0, \quad 0 \leq r \leq r_u, \quad (8a)$$

$$z_l \leq z \leq z_u,$$

$$\frac{\partial F_s}{\partial r} = \frac{\partial C_{cs}}{\partial r} = \frac{\partial C_{cg}}{\partial r} = 0, \quad t > 0, \quad r = 0, \quad r = r_u, \quad (8b)$$

$$\frac{\partial F_s}{\partial z} = \frac{\partial C_{cs}}{\partial z} = \frac{\partial C_{cg}}{\partial z} = 0, \quad t > 0, \quad z = z_l, \quad z = z_u, \quad (8c)$$

$$F_s = F_s(t), \quad C_{cs} = C_{cg} = C_{c0}, \quad t > 0, \quad (8d)$$

at the injection points,

where z_l and z_u are the lower and upper boundaries in elevation, respectively, and r_u is the upper boundary in radial direction. The soil properties and parameter values used for all simulations are provided in Tables 1 and 2, respectively.

Results and discussions

This study is to investigate the applicability of an injection method using vertical pipes in forming

Table 2 Parameter values used in numerical experiments

Parameters	Fig. 1	Fig. 3	Fig. 4a	Fig. 4b	Fig. 5a	Fig. 5b
C_{n0} (g cm ⁻¹) ($t_{0.5}$ (h)) ^a	0.02 (0.02)	0.02 (0.02)	0.015 (0.16) 0.014 (0.25) 0.012 (0.75)	0.014 (0.25)	0.012 (0.75) 0.010 (2.67) 0.009 (5.59)	0.012 (0.75)
k_0 (cm ⁻²)	2.04×10^{-6}	2.04×10^{-7}	2.04×10^{-6}	2.04×10^{-6}	2.04×10^{-7}	2.04×10^{-7}
H_i (m)	0.1	0.1	10	5 10 15	10	5 10 15
α_L (cm), α_T (cm)	1, 0.1	1, 0.1	10, 1	10, 1	10, 1	10, 1

^a This value is calculated by using Eqs. 3 and 4. In all computations, $C_{c0} = 0.39$ g cm⁻¹ and $H_0 = -9.225$ cm (i.e., $\theta_0 = 0.15$). For the simulation for the model verification, $r_u = 1.2$ m, $z_1 = -1.3$ m and $z_u = 0.3$ m. For laboratory scale simulations, $r_u = 6$ m, $z_1 = -15$ m, and $z_u = 7$ m

horizontal barrier. A gelling liquid is injected at single injection point through the vertical pipes placed in zig-zag fashion so that the gel bulb generated from each pipe could be overlapped each other. Illustrative examples with three vertical pipes (Fig. 3) demonstrate that the overlapping of the gel bulb from each injection pipe and formation of a continuous horizontal barrier can be achieved with the higher soil permeability, and/or higher injection pressure, and/or slower gelation rate of the gelling liquid (i.e., lower NaCl concentration of CS solution).

Based on these preliminary simulation results, investigation was made into the generation of a single CS gel bulb from one injection pipe at various ranges of the intrinsic soil permeability, injection pressure head, and gelation rate of the gelling liquid. The lateral extent of the barrier generated from a single CS bulb was evaluated for different gel-points (i.e., different NaCl concentrations of the solution) and injection pressure heads for two types of soils with different initial intrinsic permeabilities. From the lateral area A of the gel formation estimated from the lateral extent, and the amount of injected CS solution calculated from the simulation, the total amount of CS solution required to produce the same lateral areal extent A as the horizontal-pipe injection system (Kim and Corapcioglu 2002b) was estimated and compared to that of horizontal-pipe system in a couple of cases.

All simulation results are presented in Figs. 4 and 5 with the cross-sectional views of the gel-saturated area at $t = 2t_{0.5}$ with an injection hole at the bottom of the pipe located at point (0, 0). Kim and Corapcioglu (2002b) suggested that the gel formation accomplished at $t = 2t_{0.5}$ as evaluation of the final performance for practical purposes. Here, the gel-point $t_{0.5}$ is the time when viscosity starts to increase rapidly, with longer gel-points being observed for the solution with lower NaCl concentrations. It can be used as a measure of gelation

rate of the solution, substituting NaCl concentration of the solution. All simulation results obtained at $t = 2t_{0.5}$ were provided as the estimates of the final behavior of the gel system for practical purposes.

The gel formation presented in Figs. 4 and 5 exhibit patterns similar to the ones obtained from the horizontal-pipe system (Kim and Corapcioglu 2002b). As shown for barriers with a horizontal-pipe system, the CS solution with higher gel-point produces a barrier which extends further in the vertical direction than in the horizontal direction, and thus the ratios of the lateral to the vertical extents of the impervious zone become lower (Figs. 4a, 5a). In Figs. 4b and 5b illustrating the barrier formation at different injection pressure heads, an increase of the lateral extent comparable to the vertical one with increasing injection heads. The ratio of the vertical extent to the lateral extent appears to keep almost the same.

Lateral extent

Using the SAS[®] System for Windows[™] (Release 6.12, SAS Institute Inc.), the overall trend of lateral extent L to the injection pressure head H_i and gel-point $t_{0.5}$ was obtained. Following correlations were with the uncertainties representing 95% confidence intervals, and L , H_i , and $t_{0.5}$ are given in units of m, m, and h, respectively.

$$L \propto (t_{0.5})^{0.16 \pm 0.07} (H_i)^{0.40 \pm 0.19} \quad \text{for } k_0 = 2.04 \times 10^{-6} \text{ cm}^2, \tag{9a}$$

$$L \propto (t_{0.5})^{0.22 \pm 0.05} (H_i)^{0.41 \pm 0.09} \quad \text{for } k_0 = 2.04 \times 10^{-7} \text{ cm}^2. \tag{9b}$$

The improvement of the operating conditions such as the increase of gel-point and/or injection pressure

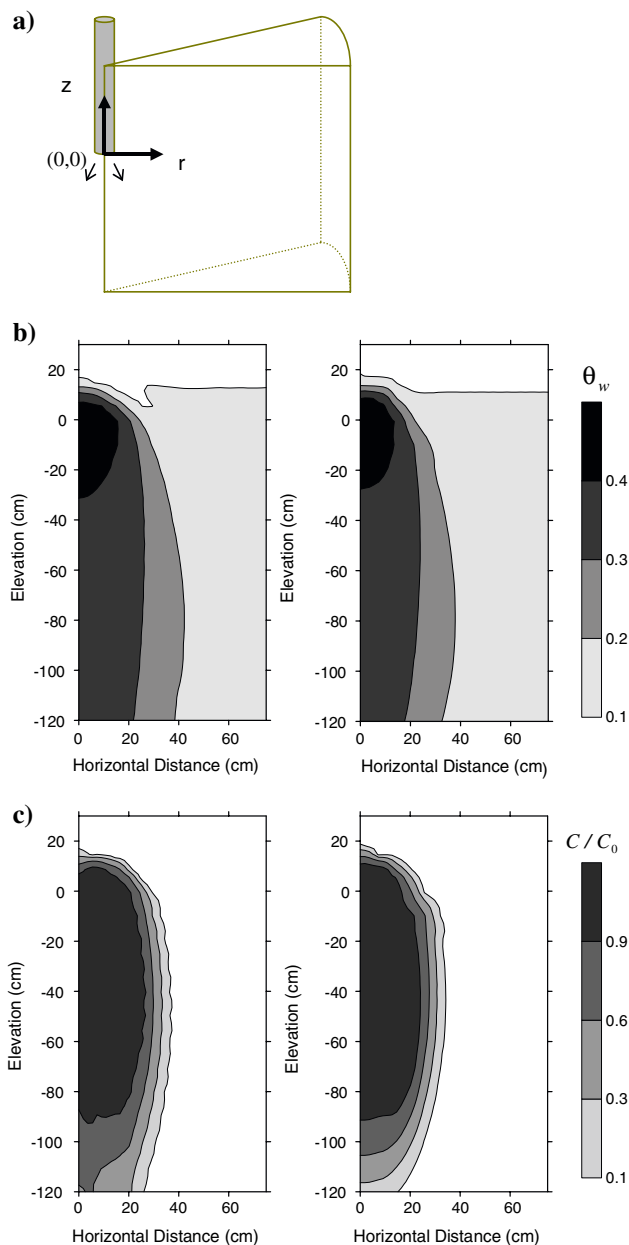


Fig. 3 **a** Schematic diagram of the point injection through a single vertical pipe (drawn not to scale); **b** distribution of water content; and **c** relative concentration profile. Left and right are the results of numerical experiments using the developed model and SWMS_2D, respectively

seems to work less effectively in the vertical-pipe system, compared to the horizontal-pipe system of Kim and Corapcioglu (2002b) in terms of the increase in the lateral extent L . In Kim and Corapcioglu, the strong dependency of L on the operating parameters, $L \propto (t_{0.5})^{0.39 \pm 0.05} (H_i)^{0.56 \pm 0.09}$ and $L \propto (t_{0.5})^{0.45 \pm 0.08} (H_i)^{0.52 \pm 0.13}$ were observed for $k_0 = 2.04 \times 10^{-6}$ and $2.04 \times 10^{-7} \text{ cm}^2$, respectively. Much lower exponents of $t_{0.5}$ and H_i in Eq. 9 seem attributable to the cylin-

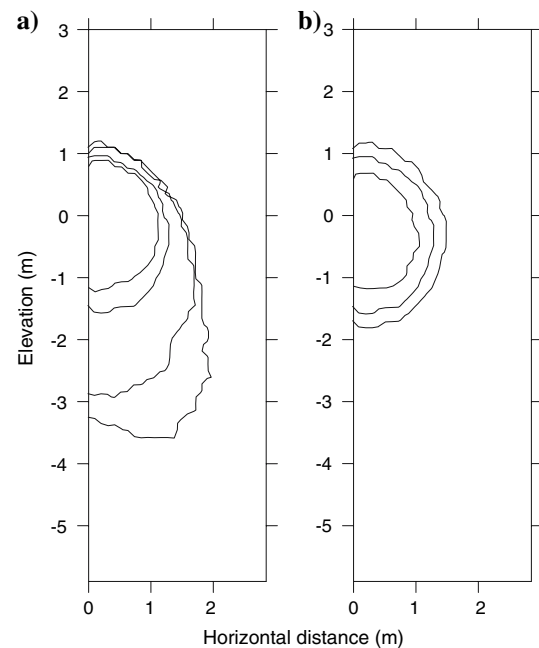


Fig. 4 Distributions of CS gel-saturated area **a** with different gel-points; **b** with different injection heads for a soil with an initial permeability of $2.04 \times 10^{-6} \text{ cm}^2$ (see Table 1 for the injection conditions)

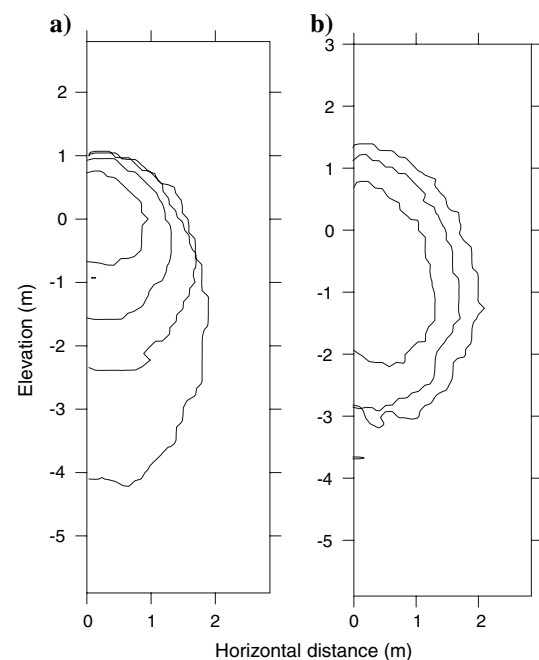


Fig. 5 Distributions of CS gel-saturated area **a** with different gel-points; **b** with different injection heads for a soil with an initial permeability of $2.04 \times 10^{-7} \text{ cm}^2$ (see Table 1 for the injection conditions)

drical symmetry associated with the CS solution injection through a vertical pipe: As the gel mixture moves in the radial direction, the specific discharge of

the gel mixture in the radial direction is likely to be reduced inversely proportional to the radial distance.

Lateral area

Due to different geometry of injection systems, a more suitable comparison can be made with the lateral area *A* of the gel formation rather than its lateral extent. Then, the dependency of the increase in the lateral area on the varying gel-point and injection pressure head was estimated and compared.

$$\left. \begin{aligned} &A \text{ (horizontal pipe)} \\ &\propto (t_{0.5})^{0.39} (H_i)^{0.56} \\ &A \text{ (vertical pipe)} \\ &\propto (t_{0.5})^{0.32} (H_i)^{0.80} \end{aligned} \right\} \text{for } k_0 = 2.04 \times 10^{-6} \text{ cm}^2, \quad (10a)$$

$$\left. \begin{aligned} &A \text{ (horizontal pipe)} \\ &\propto (t_{0.5})^{0.45} (H_i)^{0.52} \\ &A \text{ (vertical pipe)} \\ &\propto (t_{0.5})^{0.44} (H_i)^{0.82} \end{aligned} \right\} \text{for } k_0 = 2.04 \times 10^{-7} \text{ cm}^2. \quad (10b)$$

In general, the vertical-pipe system appears to be having a stronger response to the injection pressure head than that of the horizontal-pipe system. With the constant injection head condition, the larger amount of the CS solution can be pushed radially in the vertical-pipe system, differently from the horizontal-pipe system in which the solution is designed to flow mostly in a horizontal direction perpendicular to the pipe length. The vertical-pipe system, as a result of the axis symmetry, allows the lateral area to increase more cooperatively at the injection pressure increased.

Lateral area per unit CS solution volume

It is difficult to compare two systems directly due to their different configurations, and different spacing and sizes of injection holes. The lateral area produced with the same amount of CS solution seems more proper for a more practical assessment of the effectiveness of the two injection methods. Then, the lateral area generated per unit solution volume was calculated for each system: For the vertical-pipe system the total lateral area was divided by the total solution volume, and for the horizontal-pipe system the lateral extent was multiplied by the pipe length which yields the unit solution volume.

In the benchmark simulation case (V-I in Table 3) a single vertical pipe yields 3.1 m² of lateral area at the consumption of about 1.1 m³ of CS solution (*t*_{0.5} =

Table 3 Lateral area per unit CS solution volume

Case	CS volume injected (m ³)	Lateral area generated (m ²)	Lateral area per unit solution volume (m ² /m ³)	Lateral extent (m)	Lateral area per unit solution volume (m ² /m ³)
V-I	1.1	3.1	2.7		
V-II	2.6	5.0	1.2		
V-III	2.2	4.7	1.9		
H-I				1.8	6.0
H-II				2.1	4.3

0.25h, *H*_i = 10 m, *k*₀ = 2.04 × 10⁻⁶ cm²). When increasing either the pipe diameter (case of V-II) or the injection pressure (case of V-III) twofold, decrease of the lateral area per unit CS volume was observed in both cases.

When the lateral area per unit CS volume was computed for a horizontal-pipe system which was numerically simulated in Kim and Corapcioglu (2002b) with the same operating conditions as case V-I, a much higher values was obtained (case of H-I). This outcome could be originated from the injection method itself, and/or from the given conditions such as pipe diameter and spacing of the injection holes which determine the injection amount at the head boundary condition. Although the lateral area per unit solution volume was decreased to 4.3 m² after increasing both the pipe diameter and injection pressure twice, it is still a relatively higher value (case of H-II).

All evaluations of the gel formation in the subsurface were made with respect to the lateral dimension, since the vertical extents of the gel-treated areas appear high enough as the horizontal barrier in all results. Numerical simulations were conducted on the assumption of homogeneous and isotropic unsaturated soils, thus it is true that this isotropy magnifies the vertical extent of the gel-treated area than real situation. The findings in this study are believed to be valid also for anisotropic soils if the CS solution is injected at the constant head condition.

Conclusions

The vertical-pipe system shows a greater sensitivity of the lateral areal extent to the enhanced operating parameters compared to the horizontal-pipe system. When the horizontal areal extents are concerned, the vertical-pipe system appears to be having a comparable response to the increase of gel-point, and even a stronger response to the increase of injection pressure head. However, a couple of test simulations show the

vertical-pipe system requires consumption of a larger volume of CS solution than the horizontal-pipe system in forming a barrier with the same lateral area.

According to the analyses in terms of the formation of lateral area and operating condition, the point injection of the vertical-pipe system seems to be less effective in forming horizontal gel barrier for the prevention of contaminant migration in unsaturated soil, compared to the injection through the pipe length of the horizontal-pipe system. The answer to the question of which system should be preferred would depend on the site conditions and other concerns such as the accessibilities of the injection systems under consideration and the overall cost. This result could be used as a general guideline in the application of gel barrier technology.

References

- Finsterle S, Moridis GJ, Pruess K, Persoff P (1994) Physical barriers formed from gelling liquids: 1. Numerical design of laboratory and field experiments, *Rep. LBL-35113*. Lawrence Berkeley National Laboratory, Berkeley, CA
- Heiser J, Sullivan T, Ludewig H, Brower J (2000) Viscous liquid barrier demonstration at the BNL LINAC isotope producer. Paper presented at the proceedings of waste management 2000 symposium, Tucson, AZ
- Jurinak JJ, Summers LE (1991) Oilfield applications of colloidal silica gel. *SPEPE* 6:406–412
- Kim M, Corapcioglu MY (2002a) Gel barrier formation in unsaturated porous media: modeling. *J Contam Hydrol* 56(1–2):75–98
- Kim M, Corapcioglu MY (2002b) Modeling of gel barrier formation by using horizontal wells. *J Environ Eng ASCE* 128(10):929–941
- Koval EJ (1963) A method for predicting the performance of unstable miscible displacement in heterogeneous media. *Trans AIME* 228:145–154
- Moridis GJ, Finsterle S, Heiser J (1999) Evaluation of alternative designs for an injectable subsurface barrier at the Brookhaven national laboratory site, Long Island, New York. *Water Resour Res* 35(10):2937–2953
- Noll MR, Bartlett C, Dochat TM (1992) In situ permeability reduction and chemical fixation using colloidal silica. Paper presented at the 1992 proceeding of the 6th national outdoor action conference on aquifer restoration, Las Vegas, NV, 11–13 May 1992
- Pearlman L (1999) Subsurface containment and monitoring systems: barriers and beyond (overview report). <http://www.epa.gov/tio/download/remed/pearlman.pdf>
- Simunek J, Vogel T, Van Genuchten MTh (1994) The SWMS_2D Code for simulating water flow and solute transport in two-dimensional variably saturated media, version 1.21., Research Report No.132, US salinity laboratory, USDA, ARS, Riverside, CA
- Yonekura R, Kaga M (1992) Current chemical grout engineering in Japan, grouting, soil improvement, and geosynthetics. In: *Proceedings of the geotechnical special publication No.30*, ASCE, pp 725–736